HHS Public Access

Author manuscript

Am J Ophthalmol. Author manuscript; available in PMC 2018 February 01.

Published in final edited form as:

Am J Ophthalmol. 2017 February ; 174: 56–67. doi:10.1016/j.ajo.2016.10.018.

Retinal microvascular network and microcirculation assessments in high myopia

Min Li[1,2], **Ye Yang**[2,3], **Hong Jiang**[2,4], **Giovanni Gregori**[2], **Luiz Roisman**[2], **Fang Zheng**[2], **Bilian Ke**[1], **Dongyi Qu**[2], and **Jianhua Wang**[2]

[1]Department of Ophthalmology, Shanghai General Hospital, Shanghai Jiaotong University School of Medicine, Shanghai, China

[2]Bascom Palmer Eye Institute, University of Miami Miller School of Medicine, Miami, FL, USA

[3]School of Optometry and Ophthalmology, Wenzhou Medical University, Wenzhou, China

[4]Department of Neurology, University of Miami Miller School of Medicine, Miami, FL, USA

Abstract

Purpose—To investigate the changes of the retinal microvascular network and microcirculation in high myopia.

Design—A cross-sectional, matched, comparative clinical study.

Participants—Twenty eyes of twenty subjects with non-pathological high myopia (28 ± 5 Years) with a refractive error of −6.31 ± 1.23 Diopters (mean ± standard deviation) and twenty eyes of twenty age- and gender-matched control subjects (30 ± 6 years) with a refractive error of −1.40 ± 1.00 Diopters were recruited.

Methods—Optical coherence tomography angiography (OCTA) was used to image the retinal microvascular network, which was later quantified by fractal analysis (box counting, Dbox, representing vessel density) in both superficial and deep vascular plexuses. The retinal function imager (RFI) was used to image the retinal microvessel blood flow velocity (BFV). The BFV and microvascular density in the myopia group were corrected for ocular magnification using Bennett's formula.

Results—The density of both superficial and deep microvascular plexuses was significantly decreased in the myopia group in comparison to the controls ($P < 0.05$). The decrease of the microvessel density of the annular zone (0.6 – 2.5 mm), measured as D_{box}, was 2.1% and 2.9% in superficial and deep vascular plexuses, respectively. The microvessel density reached a plateau from 0.5 mm to 1.25 mm from the fovea in both groups, but that in myopic group was about 3%

*Corresponding Author: Jianhua Wang, MD, PhD, Mailing address: Department of Ophthalmology Bascom Palmer Eye Institute, 1638 NW 10th Avenue, McKnight Building - Room 202A, Miami, FL 33136, Tel: (305) 482-5010, jwang3@med.miami.edu.

Financial Disclosures

All other authors have no proprietary interest in any materials or methods. All other authors of the manuscript have no proprietary interest in any materials or methods described within this article.

lower than the control group. No significant differences were detected between the groups in retinal microvascular BFV in either arterioles or venules ($P > 0.05$). Microvascular densities in both superficial ($r = -0.45$, $P = 0.047$) and deep ($r = -0.54$, $P = 0.01$) vascular plexuses were negatively correlated with the axial lengths in the myopic eye. No correlations were observed between BFV and vessel density ($P > 0.05$).

Conclusions—Retinal microvascular decrease was observed in the high myopia subjects, whereas the retinal microvessel BFV remained unchanged. The retinal microvascular network alteration may be attributed to ocular elongation that occurs with the progression of myopia. The novel quantitative analyses of the retinal microvasculature may help to characterize the underlying pathophysiology of myopia and enable early detection and prevention of myopic retinopathy.

Keywords

retina; high myopia; microvascular network; microcirculation; retinal function imager (RFI); OCT angiography (OCTA)

Myopia, the leading cause of distance vision impairment, is a common type of refractive error that affects more than 1.4 billion people worldwide.[1] Associated with an increased risk of blindness,[2] this disorder predominantly affects young people, especially in Asia.[1] The prevalence of high myopia, a severe form of this disorder, has increased by 8-fold in the past 30 years for young and middle-aged adults in the United States.[3] High myopia can lead to myopic retinopathy, which presents with lacquer crack formation, choroidal neovascularization and chorioretinal atrophy.[4,5] These complications are highly associated with retinal vessel morphological alterations, such as narrower arterioles, which are visible on fundus photography.[4,5] Moreover, decreased choroidal blood flow has been associated with increasing axial length (AL), a possible indication of progressive myopia,[6] in both form deprivation and negative lens-induced myopic chick models.[7,8] In highly myopic patients, reduced retinal vessel density[9] and blood flow[10] were evident in the retinal large vessels visible on fundus photo. Using the Dynamic Vessel Analyzer,[11] it was found that there was a narrowing of retina large vessels, but their function was still comparable to controls.[11] The retinal capillary network and microcirculation directly supply the oxygen and nutrients to the retinal tissue, which may be more susceptible to myopia-related alterations. Understanding the changes and interaction between the retinal capillary network and microcirculation may reveal the underlying pathophysiology of the disorder and may lead to the development of better prevention and treatment. Investigating the retinal microvascular characteristics in high myopia prior to retina damage may also enable the early detection of myopic retinopathy. However, due to the technical difficulties of imaging these retinal microvessels and microcirculation and the inability to visualize them with fundus photography, myopia-related vascular changes in the micrometer level have not been characterized. This may prevent researchers from investigating them as early indicators of the onset of retinopathy.

With the FDA-approved optical coherence tomography angiography (OCTA) and Retinal Functional Imager (RFI), the retinal capillary network and microcirculation can be measured non-invasively. OCTA is an advanced ophthalmic imaging technique that can measure the vessel network in different layers of the retina structure without the use of contrast agents,

such as fluorescent dye.[12,13] It has been used to characterize retinal vascularization morphology in healthy eyes,[14] and in a number of ocular diseases, such as diabetic retinopathy, age-related macular degeneration, glaucoma, and central serous chorioretinopathy.[15] OCTA once demonstrated the choroidal neovascularization in myopic eyes with retinopathy.[16] RFI is an optical imaging device capable of measuring retinal microcirculation in pre-capillary arterioles and post-capillary venules.[17,18] This device has been used to measure retinal blood flow velocity (BFV) in a number of common ocular diseases[19–22] but has not been utilized in myopia research. Using these two advanced ophthalmic imaging devices, the goal of the present study was to characterize the retinal microvasculature and microcirculation in high myopia without retinopathy.

Methods

The present study was approved by the research review board of the University of Miami. Informed consent was obtained from each subject, and all subjects were treated in accordance with the tenets of the Declaration of Helsinki. Twenty eyes of twenty subjects with high myopia (5 males and 15 females with an average age of 28 ± 5 years (mean ± SD), Table 1) and twenty eyes of twenty age- and gender- matched controls (7 males and 13 females with an average age of 30 ± 6 years) were imaged. The high myopia subjects had a refractive error greater than −5 diopters and the healthy controls had a refractive error less than −3 diopters. Refraction data were converted to spherical equivalent (SE), which was calculated as the spherical dioptric power plus one-half of the cylindrical dioptric power. The ophthalmic examinations of all subjects were normal, without any signs of retinopathy. The best-corrected visual acuity was 20/20. None of the subjects had significant ocular or systemic disorders (or medication use) that might affect the systemic or ocular vasculature. The axial length (AL) was measured using the IOLMaster (Zeiss 500, Carl Zeiss Meditec, Inc, Dublin, CA) and the refractive diopter was measured by a standard phoropter.

The Zeiss HD-OCT with Angioplex™ OCTA device (Carl Zeiss Meditec, Dublin, CA) was used. Its technical aspects have been previously described in detail.[23] Briefly, the system is an upgrade of the Cirrus model 5000 instrument, which is capable of scanning at a rate 68,000 A-scans per second and non-invasively captures depth-encoded vasculature in the retina. The angiography is generated by repeated B-scans at the same locations and analyzed from both intensity and phase information. The algorithm for processing the blood flow information is OCT Microangiography-Complex (OMAG^c), which yields the enface vessel network in different retinal layers. In the present study, a 3 × 3 mm^2 angiogram was generated in less than 3 seconds by taking four sequential B-scans in each y-axis location with approximately 9,000 B-scans, each being composed of 245 A-scans (A scan = 1 pixel). The OCTA system is also incorporated with a real time retinal tracking technology named FastTrac™ which ensures achievement of retinal angiographic images with minimal movement artifacts.[23] Angiograms of the superficial vascular plexus and deep vascular plexus were exported for processing and analysis. The superficial vascular plexus is the term used to refer to the vascular network from the internal limiting membrane (ILM) to the inner plexiform layer (IPL), while the deep vascular plexus refers to the vascular network from the inner nuclear layer (INL) to the outer plexiform layer (OPL).[23] The vascular enface view

images of these plexuses were exported for further analysis, including magnification correction, separation of large and small vessels and fractal analysis.

The magnification for imaging the fundus using fundus photography and OCT is different in the myopic eye due to the elongation of the eye. Hence, the proper magnification correction is required for evaluating dimensional information of the retina.[24,25] The correction is often performed using keratometry measurements or axial length.[25] The Bennett's method using the axial length as the main correction factor is more accurate than the method using keratometry.[26] In the present study, Bennett's formula was used to determine a scaling factor of the OCT angiograms for adjustment of the ocular magnification in the high myopia group (scaling factor = 3.382 × 0.013062 × [AL-1.82]).[25]

The OCTA original images with a image size of 245 × 245 pixels was resized to 1,024 × 1,024 pixels to meet the image size requirement of a previously developed software program for vessel segmenation.[27,28] The images of the myopic eyes were then adjusted by the scaling factor from Bennett's formula, which produced an enlarged image with more pixels. The enlarged image was trimmed to the pixel size of 1,024 × 1,024 pixels as the corrected image (Fig. 1). To remove the large vessel from the microvascular network, the segmentation software, running in the Matlab environment (The Mathworks, Inc, Natick, MA, USA), applied a series of image processing procedures such as inverting, equalizing and the removing background noise and non-vessel structures to create a binary image. From the binary image, any vessel with a diameter ≥ 25 μm was defined as the large vessels and separated from the remaining vessels, defined as the microvessels. This procedure also eliminated the projection artifact (i.e., shadowgraphic projection artifact) of the large vessels in the superficial vascular plexus on the deep vascular plexus.[29] The microvessels were then skeletonized and partitioned. The software detected the center of the foveal avascular zone (FAZ) by searching the intensity gradient from the image center to the periphery. The center of the FAZ was used for quadrantal and annular partition. After removing the avascular zone (diameter = 0.6 mm) centered on the fovea, the annulus from 0.6 mm to 2.5 mm in diameter was defined as the annular zone with a bandwidth of 0.95 mm. The annular zone was divided by vertical and horizontal meridians into four quadrantal zones, named superior temporal (ST), inferior temporal (IT), superior nasal (SN) and inferior nasal (IN). The image from the left eye was flipped horizontally for matching of the quadrantal definition and averaging. In addition, the annular zone was divided into 6 thin annuli with a bandwidth of ~0.16 mm (Fig. 2). In addition, we manually outlined FAZ of the superficial vascular plexus images using ImageJ (Ver. 1.48, National Institutes of Health, Bethesda, MD). The operator (ML) drew the contour of the area where no vessels were present and the program calculated the area.

Further calculation was performed to obtain the diameter from the area results, assuming the FAZ was a round area. Fractal analysis was performed in each partition using the box counting method with the fractal analysis toolbox (TruSoft Benoit Pro 2.0, TruSoft International Inc, St. Petersburg, FL). In the fractal analysis software, the pixel size of the largest box for counting non-empty boxes was set to 104 pixels and the incremental rotation degree of the grid in searching non-empty boxes was set to 15 degrees, according to the

default settings. Fractal dimension (D_{box}) was obtained to represent vessel density in each zone.

The RFI system (RFI 3000, Optical Imaging Ltd., Rehovot, Israel) is a US Food and Drug Administration (FDA) approved ophthalmic imaging modality that has been well-described in the literature.[18,28,30,31] The measurement procedure of retinal microcirculation using the RFI system has been described in detail previously.[18,31–33] RFI applies a stroboscopic light source and a high-resolution digital camera to rapidly take a series of retinal images. Using hemoglobin in red blood cells as the intrinsic motion contrast agent, the system measures the velocity of the red cell clusters in pre-capillary arterioles and post-capillary venules. No external contrast agent is needed and the imaging procedure is non-invasive. The reproducible measurement is approximately 7.5%–11.0%.[34] In the present study, each participant was asked to relax for 15 minutes in a semi-dark waiting room before imaging. The pupil was dilated with 1% tropiamide and the macular region, centered on the fovea, was imaged (20 degrees with the field of view of 4.3 × 4.3 mm^2).[32] More than four well-focused images were obtained from each eye in the 20 degree camera settings for calculating blood flow velocity. Vessels were manually marked using the proprietary software in the RFI. Blood flow velocities of the arterioles and venules were automatically calculated (Fig. 3). The blood flow velocity in myopic eyes was adjusted for ocular magnification using the same scaling factor as the OCTA image correction and calculated as the measured velocity × the scaling factor.

All data were analyzed with the statistical package (Statistic, StatSoft, Inc, Tulsa, OK) and presented in the format of mean ± standard deviation (SD). The repeated measurement analysis of variance (Re-ANOVA) was used for overall effects for annular and quadrantal results between groups. Post hoc tests with Tukey correction were used to determine the existence of pairwise differences between different zones and groups. Independent sample t-tests were used to assess biographic and annular (0.6 – 2.5 mm) differences between the groups. Correlations between macular vessel density and AL and refraction were determined using the Pearson's correlation test. A P-value of < 0.05 was considered statistically significant.

Results

The demographic and clinical information of subjects in the two groups are listed in Table 1. There were no significant differences in age or gender ($P > 0.05$) between the myopia subjects and the healthy controls. Significant differences between groups were found in axial length and refraction ($P < 0.05$). The microvessel density of the annular zone (0.6 – 2.5 mm), measured as D_{box}, of both superficial and deep vascular plexuses was significantly lower in the myopia group than in the control group ($P < 0.01$, Fig. 4 and 5, Table 2). The decrease of the microvessel density of the annular zone (0.6 – 2.5 mm), measured as D_{box}, was 2.1% and 2.9% in superficial and deep vascular plexuses, respectively.

The microvessel density in the thin annuli from C2 (i.e., 0.5 mm from the fovea) to C6 (1.25 mm from the fovea) was significantly lower in the myopia group compared to the control group ($P < 0.05$, Table 2, Fig. 5), except for C2 in the deep vascular plexus. The microvessel

density reached a plateau from C2 to C6 in both groups, but that in myopic group was about 3% lower than the control group. Analysis of quadrantal partitions showed significant decreases in all quadrants in both plexuses, with the exception of the ST quadrant ($P < 0.05$, Table 3, Fig. 5).

The FAZ area was 0.28 ± 0.12 mm^2 in myopia group, which was not significantly different compared to the control group (0.28 ± 0.13 mm^2, $P > 0.05$). The calculated FAZ diameter in the myopia group was 0.59 ± 0.12 mm, which was not significantly different compared to the control group (0.58 ± 0.12 mm, $P > 0.05$).

When evaluating the retinal microcirculation, the myopia subjects had an average retinal arteriolar BFV of 3.67 ± 0.48 mm/s and an average venular BFV of 3.06 ± 0.47 mm/s. In the healthy controls, the average retinal arteriolar BFV was 3.70 ± 0.43 mm/s and the average venular BFV was 2.95 ± 0.25 mm/s. There were no significant differences in retinal arteriolar or venular BFV between the myopia subjects and the controls ($P = 0.44$, 0.18).

Microvascular density in both superficial and deep vascular plexuses was negatively correlated with AL and refractive diopters when the results of both groups were combined (Fig. 6). When the densities were analyzed separately, microvascular densities in both superficial ($r = -0.45$, $P = 0.047$) and deep ($r = -0.54$, $P = 0.01$) vascular plexuses were negatively correlated with the axial lengths in the myopic eye. Interestingly, microvascular densities in the superficial vascular plexus ($r = -0.52$, $P = 0.02$) were negatively correlated to the refractive diopter in the control group. No significant correlation was detected between BFV and either of the two factors (i.e., axial length and refraction) or between the vessel density and BFV ($P > 0.05$).

Discussion

To the best of our knowledge, this study is the first to explore both the microvascular network density and microcirculation in highly myopic eyes without noticeable degenerative retinopathy. The present study primarily determined that the retinal capillary density decreases in highly myopic patients with normal visual ability prior to permanent retinal damage. Based on the correlation analysis, this alteration appeared to become more prominent in the presence of axial length elongation and higher refractive diopter, the clinical markers of worsening myopia. These observations mirror the results observed in the retinal large vessels of myopic young adults, as reported by Azemin et al. using fundus photography.[9] It can be speculated that, with the progress of myopia, the structural elongation of the eyeball mechanically stretches the retinal tissue, resulting in the decrease of the retinal microvascular density. The trend of which was similar to the decreased vascular endothelial growth factor (VEGF) which was found to have a negative correlation with the axial length.[35–37] VEGF produced by vascular endothelial cells and retinal pigment epithelium (RPE) cells, may play a key role in the development of retinal vasculature by stimulating the vessel growth.[35,38,39] The decreased aqueous VEGF level found in high myopia may also contribute to the possible loss of capillary network.[29,31] It is possible that, with the progress of myopia, the thinned retina due to the elongated axial length can cause

the degeneration of retinal vascular endothelial cells and retinal pigment epithelium (RPE) cells, resulting in consequential decreases in VEGF production and microvessel density.

Fractal analysis is commonly used to quantify the vascular network in fundus images,[40–47] and the approach has been reliably used to analyze large retinal vessel density quantitatively in myopic eyes.[45,46] We adapted fractal analysis to analyze the microvessel network in a non-invasive capillary network, acquired using a Retinal Function Imager (RFI).[27,28] The variability of the fractal analysis for the microvessel network is 0.8% for box counting.[28] Our previous study successfully showed retinal microvascular impairment in patients with multiple sclerosis (MS), with a significant decrease in fractal dimension (0.54%).[27] In the present study, the D_{box} difference of the superficial vascular plexus annulus (0.6–2.5 mm) between groups was 2.9%, which is larger than previous findings in other conditions by others[43,48,49] and us.[27] Previous studies using fractal analysis of the retinal vessel tree showed small magnitudes in the changes in the fundus images, which were statistically significant in patients with diabetic retinopathy (0.56%), cognitive dysfunction (0.87%), and stroke (0.3%) compared to controls.[43,48,49] In contrast, using vessel density analysis, Pinhas et al. documented approximately 20% of retinal vessel alteration in patients with diabetic retinopathy.[50] The magnitude of the changes in fractal dimension (no unit) cannot be directly compared with the changes in vessel density (unit %). Vessel density calculation often calculates the pixels with vessel coverage, which is dependent on vessel width.[50] In the other words, large vessels carry more weight in the calculation. By skeletonizing the vessels, as we did in the present study, larger vessels were removed and all microvessels were thinned to one pixel line. Skeletonization is commonly used in fractal analysis of vessel trees and the box count method is used to indicate the vessel density.[40–44] Fractal analysis with skeletonization may be suitable for quantitatively analyzing microvessel networks acquired using OCTA, which contains mainly the capillaries. Further studies are warranted to test the comparability between fractal dimension and vessel coverage rate (i.e., vessel density). While we documented the changes in fractal dimension in the annulus without the center 0.6 mm foveal zone, we did not identify any difference in the area and diameter of the FAZ. This finding may indicate that the FAZ may not be a location for studying the changes of the microvessel network density in myopic eyes.

The superficial vascular plexus mainly supplies blood flow to the retinal nerve fiber layer (RNFL) and ganglion cell layer (GCL), and its distribution is not even from the edge of the FAZ to the parafoveal region.[27] The density reached a plateau from C2 (i.e., 0.5 mm from the fovea) to C6 (1.25 mm from the fovea), corresponding to the GCL thickness profile. A large variation was found in the C1 annulus, mainly due to the individual deviation of the FAZ. In the myopic eyes, the alterations in the microvessel network appeared to be similar from the annulus C2 to C6 for both plexuses, and no significant changes in the annulus C1 were found. In contrast to the evenly distributed vessel density in quadrants in the control group, quadrantal alterations in the myopia group were not even, with the biggest changes noted in the inferior nasal sector. It could be speculated that the changes in vessel density in the inferonasal sector may be due to the loss of the nerve fiber layer (i.e., peripapillary atrophy, often on the temporal side of the optic disk) in the corresponding area, which is the inferotemporal sector to the optic nerve head, which is evident in myopic normal-tension glaucoma.[51] However, this viewpoint warrants further investigation.

On the other hand, we did not find significant differences in the retinal microvascular BFV between high myopic subjects and age- and gender- matched controls, which is in agreement with the changes of the microretinal blood flow, velocity and volume in young healthy myopes measured with the Heidelberg retina flowmeter.[52] The unchanged velocity in the macular microvessels in the healthy myopic eyes found in the present study is also in agreement with a previous study by Shimada et al., who used laser Doppler flowmeter with ocular magnification correction, and found that the retinal blood flow velocity in the retinal central arteries remained unaltered in mild and high myopic eyes.[10] Furthermore, Benavente-Perez et al. also reported reduced end diastolic velocity in the central retinal arteries in high myopes, however, the peak systolic velocity remained unchanged.[52] Due to the narrowing of the retinal large vessels,[10] Shimada et al. documented reduced blood flow in the retinal central arteries in high myopic eyes. While the narrowing of the retinal large vessel caliber in myopic eyes (visible on fundus photos) is well documented,[11,53] it is still not clear whether the microvessel diameter is altered while the velocity level is maintained in myopic eyes. Evidence shows that the overall perfusion is maintained, regardless of the decreased end diastolic velocity,[52] while the density of the microvessel network is reduced, as is evident in the present study. This finding may indicate that the microvessel network maybe stretched, rather than lost. It could also be speculated that with the worsening of myopia, the eyeball is being stretched and elongated, eventually resulting in reduced ocular perfusion. Autoregulation of retinal microcirculation may be another explanation for unchanged microvessel blood velocity. The autoregulation in the retina could maintain continuous and sufficient blood flow to ensure the function of the retinal tissue despite the change of local factors, such as metabolic and CO_2.[54,55] Unlike the outer retina, which mainly gets nutrients from the choroidal blood flow, the inner retina is mainly supplied by the retinal microvasculature. It is possible that the retinal microcircular autoregulation could still maintain the retinal microvascular velocities in the early high myopia stage (without myopic retinopathy), while the density of the microvessel network decreases. Further studies in pathological myopia may help better understanding the changes of the retinal microvasculature and microcirculation in high myopia. Furthermore, we noted that microvascular densities in both superficial and deep vascular plexuses in the control group were significantly related to refractive errors, not axial lengths. We suspect that the refractive error alone may play a role in the alteration of retinal microvascular density, which may represent a different mechanism compared to what happens in the highly myopic eyes. Further studies with a large sample size may confirm the relation.

There are limitations to the present study. Due to the resolution limitation of the digital camera in the RFI system, the information about microvessel diameter is not available, which limited the interpretation of the blood flow in these measured microvessels. OCTA is also limited in resolution for the scanned area, which may not be used to measure the vessel diameters. In the present study, we focused on the early stage of the healthy myopes and did not include the eyes with myopia-related retinopathies. Our results showed the alteration of the retinal microvessel density, but no significant changes in retinal blood flow velocity. Further longitudinal studies may address the question of whether retinal microcirculation is altered with the progression of high myopia. Our current segmentation software only detects the center of the fovea using intensity gradient, while the FAZ was manually outlined.

Further development is needed to automatically determine the boundaries of the FAZ. Lastly, the sample size may be too small, although significant differences were found in retinal microvessel density. Using the software program GPower (Ver. 3.1.9),[56] we calculated the sample size based on the differences in the annular microvessel network results and the calculation indicated that we only need to have 18 cases in each group to determine the true difference of the vessel density with a detection power of 90%. Therefore, our sample size may be sufficient for determining the vessel density differences between groups. In the present study, two distinct populations (myopic and healthy) were recruited with no overlapping of refractive errors, although they overlapped for axial length. Computing Pearson correlation coefficient with the vessel density might not be appropriate for refractive error. Further large scale studies are needed establish the relationship between the axial length with possible weighted sampling on refractive error.

In summary, we characterized the retinal microvasculature and microcirculation in high myopia without retinopathy. The retinal microvessel density was altered in both superficial and deep vascular plexuses, while the retinal microvessel blood flow velocity remained unchanged. The changes in vessel density were related to axial length, indicating that the microvessel network may be stretched due to the ocular elongation in high myopic eyes. The novel quantitative analysis of the retinal microvasculature may increase understanding of the underlying pathophysiology of myopia and enable early detection and prevention of the onset of myopic retinopathy.

Supplementary Material

Refer to Web version on PubMed Central for supplementary material.

Acknowledgments

Funding / Support

This research was supported by the National Multiple Sclerosis Society, NIH Center Grant P30 EY014801, and a grant from Research to Prevent Blindness (RPB).

Dr. Jianhua Wang is a member of scientific advisory board of Optical Imaging Ltd.

Other Acknowledgments

The authors wish to thank Ms. Liang Wang from Johns Hopkins University, Baltimore, MD for assistance in preparing the manuscript and editing.

Design of the study (ML, YY, HJ, JW); data collection (ML, YY, JW, GG, LR, FZ, DQ); analysis and interpretation of the data (ML, YY, HJ, JW, GG, LR, FZ, BK, DQ); preparation, review and approval of the manuscript (ML, YY, HJ, JW, BK, DQ).

References

1. Holden BA, Fricke TR, Wilson DA, et al. Global Prevalence of Myopia and High Myopia and Temporal Trends from 2000 through 2050. Ophthalmology. 2016; 123(5):1036–1042. [PubMed: 26875007]
2. Williams KM, Hysi PG, Nag A, Yonova-Doing E, Venturini C, Hammond CJ. Age of myopia onset in a British population-based twin cohort. Ophthalmic Physiol Opt. 2013; 33(3):339–345. [PubMed: 23510367]

3. Vitale S, Sperduto RD, Ferris FL III. Increased prevalence of myopia in the United States between 1971–1972 and 1999–2004. Arch Ophthalmol. 2009; 127(12):1632–1639. [PubMed: 20008719]
4. Li H, Mitchell P, Rochtchina E, Burlutsky G, Wong TY, Wang JJ. Retinal vessel caliber and myopic retinopathy: the blue mountains eye study. Ophthalmic Epidemiol. 2011; 18(6):275–280. [PubMed: 22053837]
5. Kim YM, Yoon JU, Koh HJ. The analysis of lacquer crack in the assessment of myopic choroidal neovascularization. Eye (Lond). 2011; 25(7):937–946. [PubMed: 21527958]
6. Meng W, Butterworth J, Malecaze F, Calvas P. Axial length of myopia: a review of current research. Ophthalmologica. 2011; 225(3):127–134. [PubMed: 20948239]
7. Shih YF, Fitzgerald ME, Norton TT, Gamlin PD, Hodos W, Reiner A. Reduction in choroidal blood flow occurs in chicks wearing goggles that induce eye growth toward myopia. Curr Eye Res. 1993; 12(3):219–227. [PubMed: 8482110]
8. Fitzgerald ME, Wildsoet CF, Reiner A. Temporal relationship of choroidal blood flow and thickness changes during recovery from form deprivation myopia in chicks. Exp Eye Res. 2002; 74(5):561–570. [PubMed: 12076077]
9. Azemin MZ, Daud NM, Ab HF, Zahari I, Sapuan AH. Influence of refractive condition on retinal vasculature complexity in younger subjects. Scientific World Journal. 2014; 2014:783525. [PubMed: 25371914]
10. Shimada N, Ohno-Matsui K, Harino S, et al. Reduction of retinal blood flow in high myopia. Graefes Arch Clin Exp Ophthalmol. 2004; 242(4):284–288. [PubMed: 14722781]
11. La SC, Corvi F, Bandello F, Querques G. Static characteristics and dynamic functionality of retinal vessels in longer eyes with or without pathologic myopia. Graefes Arch Clin Exp Ophthalmol. 2015; 254(5):827–834. [PubMed: 26245340]
12. Teussink MM, Breukink MB, van Grinsven MJ, et al. OCT Angiography Compared to Fluorescein and Indocyanine Green Angiography in Chronic Central Serous Chorioretinopathy. Invest Ophthalmol Vis Sci. 2015; 56(9):5229–5237. [PubMed: 26244299]
13. Zhang Q, Lee CS, Chao J, et al. Wide-field optical coherence tomography based microangiography for retinal imaging. Sci Rep. 2016; 6:22017. [PubMed: 26912261]
14. Savastano MC, Lumbroso B, Rispoli M. In vivo characterization of retinal vascularization morphology using optical coherence tomography angiography. Retina. 2015; 35(11):2196–2203. [PubMed: 25932558]
15. de Carlo T, Romano A, Waheed N, Duker J. A review of optical coherence tomography angiography (OCTA). International Jouirnal of Retina and Vitreous. 2015; 1(5):1–15.
16. Miyata M, Ooto S, Hata M, et al. Detection of Myopic Choroidal Neovascularization Using Optical Coherence Tomography Angiography. Am J Ophthalmol. 2016; 165:108–114. [PubMed: 26973049]
17. Nelson DA, Burgansky-Eliash Z, Barash H, et al. High-resolution wide-field imaging of perfused capillaries without the use of contrast agent. Clin Ophthalmol. 2011; 5:1095–1106. [PubMed: 21887088]
18. Landa G, Jangi AA, Garcia PM, Rosen RB. Initial report of quantification of retinal blood flow velocity in normal human subjects using the Retinal Functional Imager (RFI). Int Ophthalmol. 2012; 32(3):211–215. [PubMed: 22484724]
19. Burgansky-Eliash Z, Nelson DA, Bar-Tal OP, Lowenstein A, Grinvald A, Barak A. Reduced retinal blood flow velocity in diabetic retinopathy. Retina. 2010; 30(5):765–773. [PubMed: 20061994]
20. Burgansky-Eliash Z, Barash H, Nelson D, et al. Retinal blood flow velocity in patients with age-related macular degeneration. Curr Eye Res. 2014; 39(3):304–311. [PubMed: 24147793]
21. Burgansky-Eliash Z, Bartov E, Barak A, Grinvald A, Gaton D. Blood-Flow Velocity in Glaucoma Patients Measured with the Retinal Function Imager. Curr Eye Res. 2016; 41(7):965–970. [PubMed: 26513272]
22. Beutelspacher SC, Serbecic N, Barash H, Burgansky-Eliash Z, Grinvald A, Jonas JB. Central serous chorioretinopathy shows reduced retinal flow circulation in retinal function imaging (RFI). Acta Ophthalmol. 2011; 89(6):e479–e482. [PubMed: 21435194]

23. Rosenfeld PJ, Durbin MK, Roisman L, et al. ZEISS Angioplex Spectral Domain Optical Coherence Tomography Angiography: Technical Aspects. Dev Ophthalmol. 2016; 56:18–29. [PubMed: 27023249]
24. Bennett AG, Rudnicka AR, Edgar DF. Improvements on Littmann's method of determining the size of retinal features by fundus photography. Graefes Arch Clin Exp Ophthalmol. 1994; 232(6):361–367. [PubMed: 8082844]
25. Moghimi S, Hosseini H, Riddle J, et al. Measurement of optic disc size and rim area with spectral-domain OCT and scanning laser ophthalmoscopy. Invest Ophthalmol Vis Sci. 2012; 53(8):4519–4530. [PubMed: 22577077]
26. Garway-Heath DF, Rudnicka AR, Lowe T, Foster PJ, Fitzke FW, Hitchings RA. Measurement of optic disc size: equivalence of methods to correct for ocular magnification. Br J Ophthalmol. 1998; 82(6):643–649. [PubMed: 9797665]
27. Jiang H, Delgado S, Liu C, et al. In Vivo Characterization of Retinal Microvascular Network in Multiple Sclerosis. Ophthalmology. 2016; 123(2):437–438. [PubMed: 26299696]
28. Jiang H, Debuc DC, Rundek T, et al. Automated segmentation and fractal analysis of high-resolution non-invasive capillary perfusion maps of the human retina. Microvasc Res. 2013; 89:172–175. [PubMed: 23806780]
29. Zhang M, Hwang TS, Campbell JP, et al. Projection-resolved optical coherence tomographic angiography. Biomed Opt Express. 2016; 7(3):816–828. [PubMed: 27231591]
30. Lopes de Faria JM, Andreazzi DD, Larico Chavez RF, Arthur AM, Arthur R, Iano Y. Reliability and validity of digital assessment of perifoveal capillary network measurement using high-resolution imaging. Br J Ophthalmol. 2014; 98(6):726–729. [PubMed: 24511082]
31. Landa G, Rosen RB. New patterns of retinal collateral circulation are exposed by a retinal functional imager (RFI). Br J Ophthalmol. 2010; 94(1):54–58. [PubMed: 19692362]
32. Jiang H, Delgado S, Tan J, et al. Impaired retinal microcirculation in multiple sclerosis. Mult Scler. 2016 Epub ahead of print.
33. Izhaky D, Nelson DA, Burgansky-Eliash Z, Grinvald A. Functional imaging using the retinal function imager: direct imaging of blood velocity, achieving fluorescein angiography-like images without any contrast agent, qualitative oximetry, and functional metabolic signals. Jpn J Ophthalmol. 2009; 53(4):345–351. [PubMed: 19763751]
34. Burgansky-Eliash Z, Lowenstein A, Neuderfer M, et al. The correlation between retinal blood flow velocity measured by the retinal function imager and various physiological parameters. Ophthalmic Surg Lasers Imaging Retina. 2013; 44(1):51–58. [PubMed: 23418734]
35. Chen W, Song H, Xie S, Han Q, Tang X, Chu Y. Correlation of macular choroidal thickness with concentrations of aqueous vascular endothelial growth factor in high myopia. Curr Eye Res. 2015; 40(3):307–313. [PubMed: 25300046]
36. Shin YJ, Nam WH, Park SE, Kim JH, Kim HK. Aqueous humor concentrations of vascular endothelial growth factor and pigment epithelium-derived factor in high myopic patients. Mol Vis. 2012; 18:2265–2270. [PubMed: 22933839]
37. Sawada O, Miyake T, Kakinoki M, Sawada T, Kawamura H, Ohji M. Negative correlation between aqueous vascular endothelial growth factor levels and axial length. Jpn J Ophthalmol. 2011; 55(4): 401–404. [PubMed: 21607685]
38. Chen J, Smith LE. Retinopathy of prematurity. Angiogenesis. 2007; 10(2):133–140. [PubMed: 17332988]
39. Noma H, Funatsu H, Yamasaki M, et al. Aqueous humour levels of cytokines are correlated to vitreous levels and severity of macular oedema in branch retinal vein occlusion. Eye (Lond). 2008; 22(1):42–48. [PubMed: 16826241]
40. MacGillivray TJ, Patton N. A reliability study of fractal analysis of the skeletonised vascular network using the "box-counting" technique. Conf Proc IEEE Eng Med Biol Soc. 2006; 1:4445–4448. [PubMed: 17946630]
41. Doubal FN, MacGillivray TJ, Patton N, Dhillon B, Dennis MS, Wardlaw JM. Fractal analysis of retinal vessels suggests that a distinct vasculopathy causes lacunar stroke. Neurology. 2010; 74(14):1102–1107. [PubMed: 20368631]

42. MacGillivray TJ, Patton N, Doubal FN, Graham C, Wardlaw JM. Fractal analysis of the retinal vascular network in fundus images. Conf Proc IEEE Eng Med Biol Soc. 2007; 2007:6456–6459. [PubMed: 18003503]
43. Talu S, Calugaru DM, Lupascu CA. Characterisation of human non-proliferative diabetic retinopathy using the fractal analysis. Int J Ophthalmol. 2015; 8(4):770–776. [PubMed: 26309878]
44. Talu S. Fractal analysis of normal retinal vascular network. Oftalmologia. 2011; 55(4):11–16. [PubMed: 22642130]
45. Azemin MZ, Daud NM, Ab HF, Zahari I, Sapuan AH. Influence of refractive condition on retinal vasculature complexity in younger subjects. Scientific World Journal. 2014; 2014:783525. [PubMed: 25371914]
46. Li H, Mitchell P, Liew G, et al. Lens opacity and refractive influences on the measurement of retinal vascular fractal dimension. Acta Ophthalmol. 2010; 88(6):e234–e240. [PubMed: 20662797]
47. Li H, Mitchell P, Rochtchina E, Burlutsky G, Wong TY, Wang JJ. Retinal vessel caliber and myopic retinopathy: the blue mountains eye study. Ophthalmic Epidemiol. 2011; 18(6):275–280. [PubMed: 22053837]
48. Aliahmad B, Kumar DK, Hao H, et al. Zone specific fractal dimension of retinal images as predictor of stroke incidence. Scientific World Journal. 2014; 2014:467462. [PubMed: 25485298]
49. Cheung CY, Ong S, Ikram MK, et al. Retinal vascular fractal dimension is associated with cognitive dysfunction. J Stroke Cerebrovasc Dis. 2014; 23(1):43–50. [PubMed: 23099042]
50. Pinhas A, Razeen M, Dubow M, et al. Assessment of perfused foveal microvascular density and identification of nonperfused capillaries in healthy and vasculopathic eyes. Invest Ophthalmol Vis Sci. 2014; 55(12):8056–8066. [PubMed: 25414179]
51. Sung MS, Kang YS, Heo H, Park SW. Optic Disc Rotation as a Clue for Predicting Visual Field Progression in Myopic Normal-Tension Glaucoma. Ophthalmology. 2016; 123(7):1484–1493. [PubMed: 27157844]
52. Benavente-Perez A, Hosking SL, Logan NS, Broadway DC. Ocular blood flow measurements in healthy human myopic eyes. Graefes Arch Clin Exp Ophthalmol. 2010; 248(11):1587–1594. [PubMed: 20502909]
53. Patton N, Maini R, MacGillivary T, Aslam TM, Deary IJ, Dhillon B. Effect of axial length on retinal vascular network geometry. Am J Ophthalmol. 2005; 140(4):648–653. [PubMed: 16140248]
54. Robinson F, Riva CE, Grunwald JE, Petrig BL, Sinclair SH. Retinal blood flow autoregulation in response to an acute increase in blood pressure. Invest Ophthalmol Vis Sci. 1986; 27(5):722–726. [PubMed: 3700021]
55. Arciero J, Harris A, Siesky B, et al. Theoretical analysis of vascular regulatory mechanisms contributing to retinal blood flow autoregulation. Invest Ophthalmol Vis Sci. 2013; 54(8):5584–5593. [PubMed: 23847315]
56. Erdfelder E, Faul F, Buchner A. GPower: a general power analysis program. Behaviour Research Methods, Instruments, & Computers. 1996; 28(1):1–11.

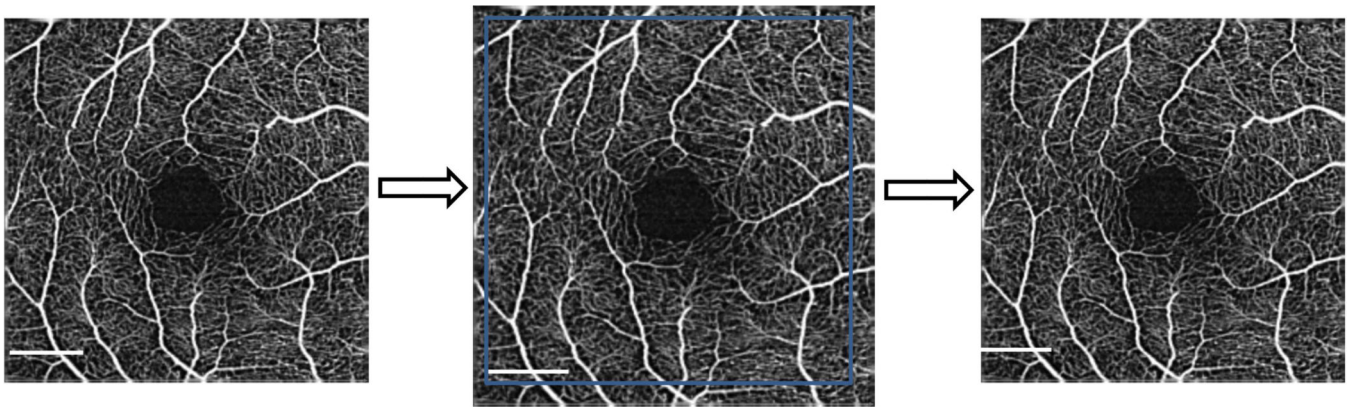

Fig. 1. Magnification correction of OCTA image

The OCTA original image with an image size of 245 × 245 pixels was resized to 1,024 × 1,024 pixels (Fig. 1 left). The resized image was then enlarged according to the scaling factor calculated using the axial length with Bennett's magnification correction formula (Fig. 1 middle). After that, the enlarged image was trimmed to 1,024 ×1,024 pixels as the corrected image for myopic eye (Fig. 1 right). Bar = 500 μm.

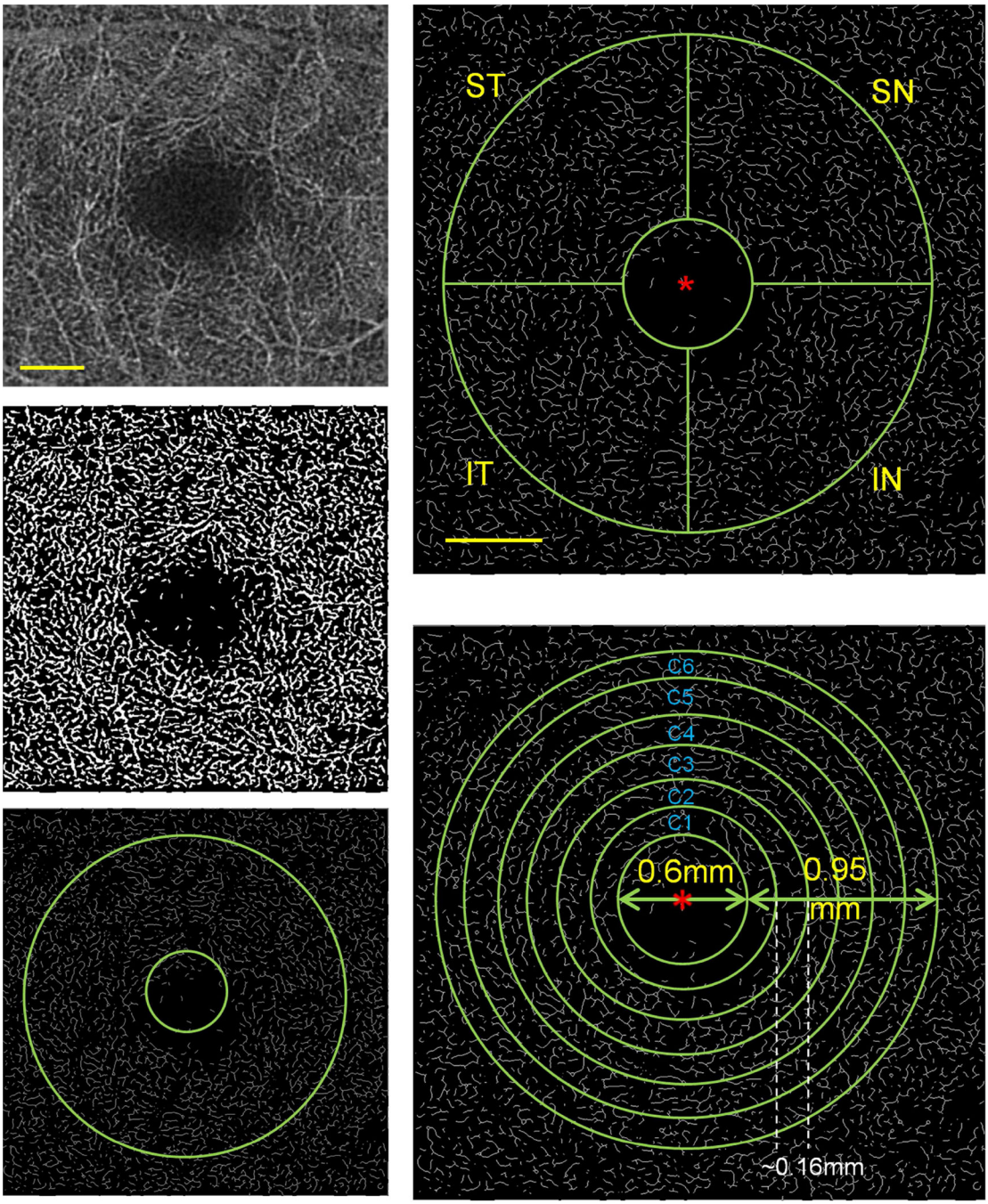

Fig. 2. Image processing and partition of retinal vessel network

To remove and separate the large vessel from the microvascular network in the superficial microvascular network and the shadowgraphic artifact (Fig. 2 upper left), custom segmentation software applied a series of image processing procedures such as inverting, equalizing and the removing background noise and non-vessel structures to create a binary image (Fig. 2 middle left). From the binary image, any vessel with a diameter ≥ 25 μm was removed and the remaining microvessels were then skeletonized (Fig. 2 bottom left). The software detected the center of the foveal avascular zone (FAZ) by searching the intensity

gradient from the image center to the periphery (Fig. 2 middle left). The center of the FAZ was used for quadrantal and annular partition (Fig. 2 upper and bottom right). After removing the avascular zone (diameter = 0.6 mm) centered on the fovea, the annulus from 0.6 mm to 2.5 mm in diameter was defined as the annular zone with a bandwidth of 0.95 mm (Fig. 2 bottom left). The annular zone was divided by vertical and horizontal meridians into four quadrantal zones, named superior temporal (ST), inferior temporal (IT), superior nasal (SN) and inferior nasal (IN) (Fig. 2 upper right). In addition, the annular zone was divided into 6 thin annuli with a bandwidth of ~0.16 mm (Fig. 2 bottom right). Bar = 500 μm.

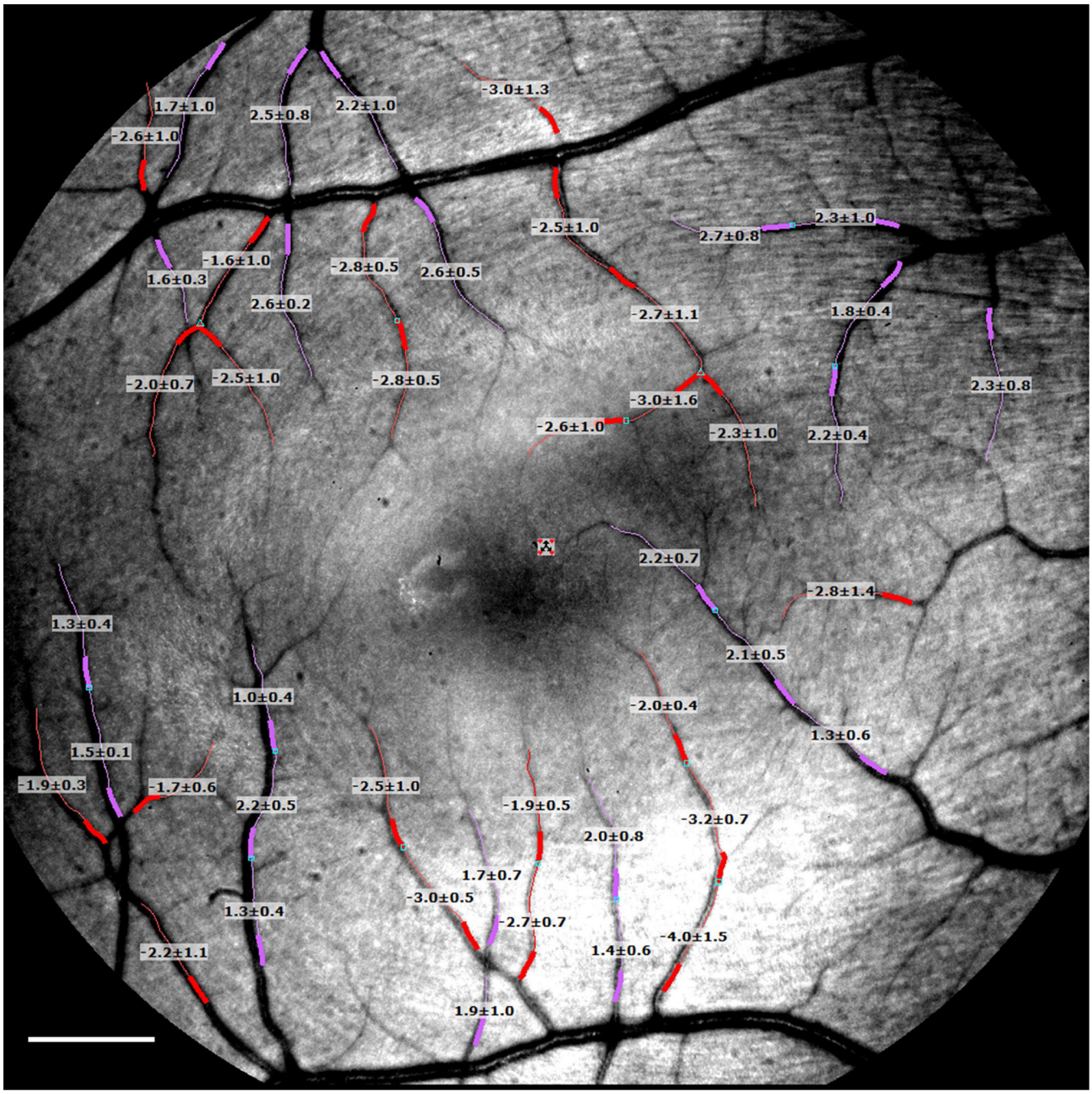

Fig. 3. Retinal blood flow velocity in arterioles and venules

The retina of a myopia subject was imaged using RFI with a field of view of 20 degrees, centered on the fovea. The secondary and tertiary branches of the retinal vessels were measured. The arterioles (marked in red) and venules (marked in purple) were labeled and read with the measured blood flow velocities (Mean ± SD: mm/s). A negative value indicates blood flow away from the heart. In this case, the arteriolar flow moved toward the fovea. A positive value indicates blood flow toward the heart. In this case, the vessels are venules. Bar = 500 μm.

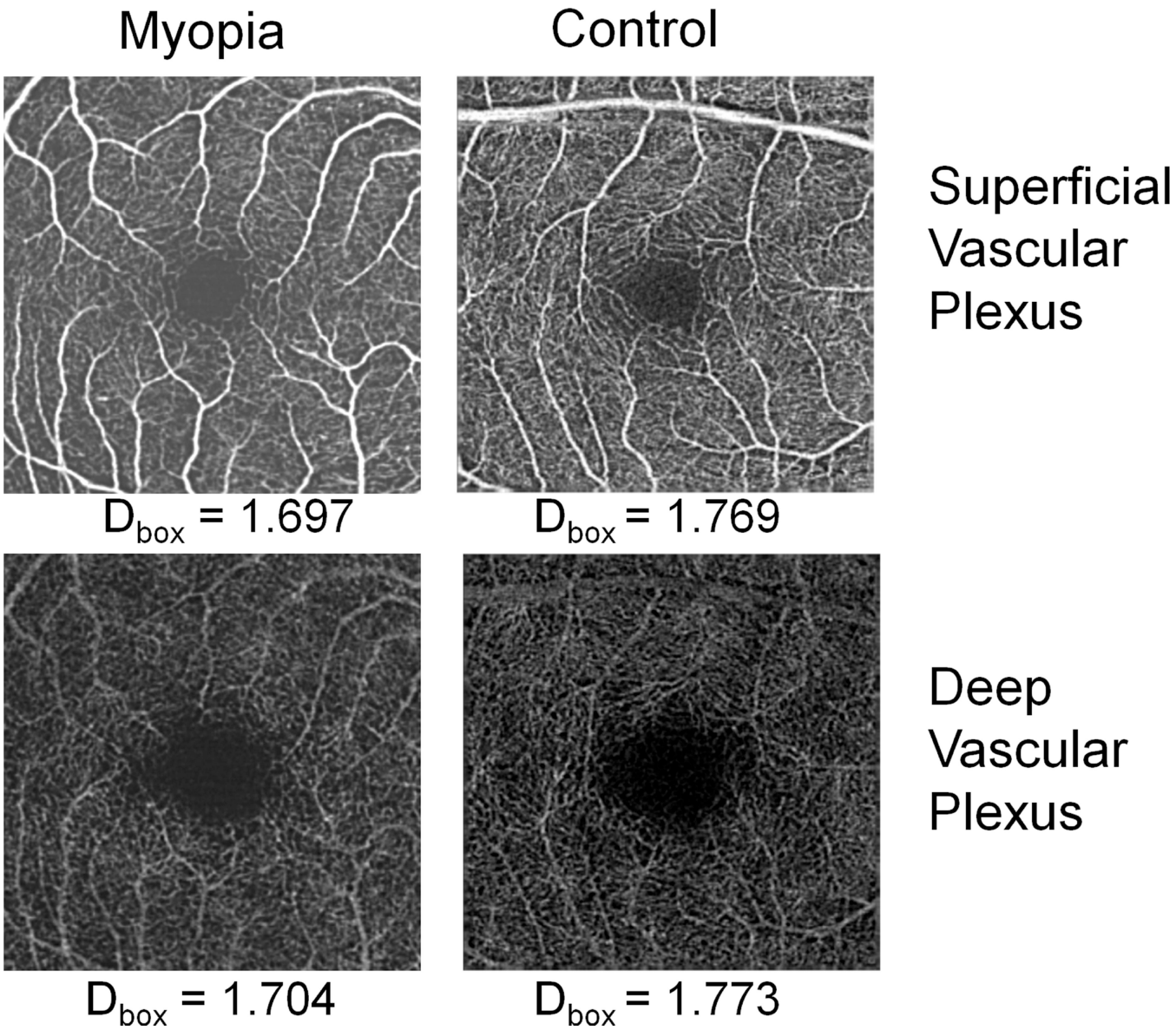

Fig. 4. Comparison of the retinal microvascular network of the myopia group and control group in superficial and deep vascular plexuses

Superficial (Fig. 4 upper left and right) and deep (Fig. 4 bottom left and right) vascular plexuses were obtained in a high myopic eye (Fig. 4 upper and bottom left) and a healthy control eye (Fig. 4 upper and bottom right). Fractal dimension (D_{box}), representing the microvascular network, was calculated after the large vessels in the superficial vascular plexus and shadowgraphic projection artifact in the deep vascular plexus were removed. D_{box} of the annulus from 0.6 to 2.5 mm in diameter is listed under each of the figures and shows decreased microvascular density in both Fig. 4 upper and bottom left of the myopic eye compared to the control eye (Fig. 4 upper and bottom right). Note: Fig. 4 bottom left and right are raw images and the shadowgraphic projection artifacts are present.

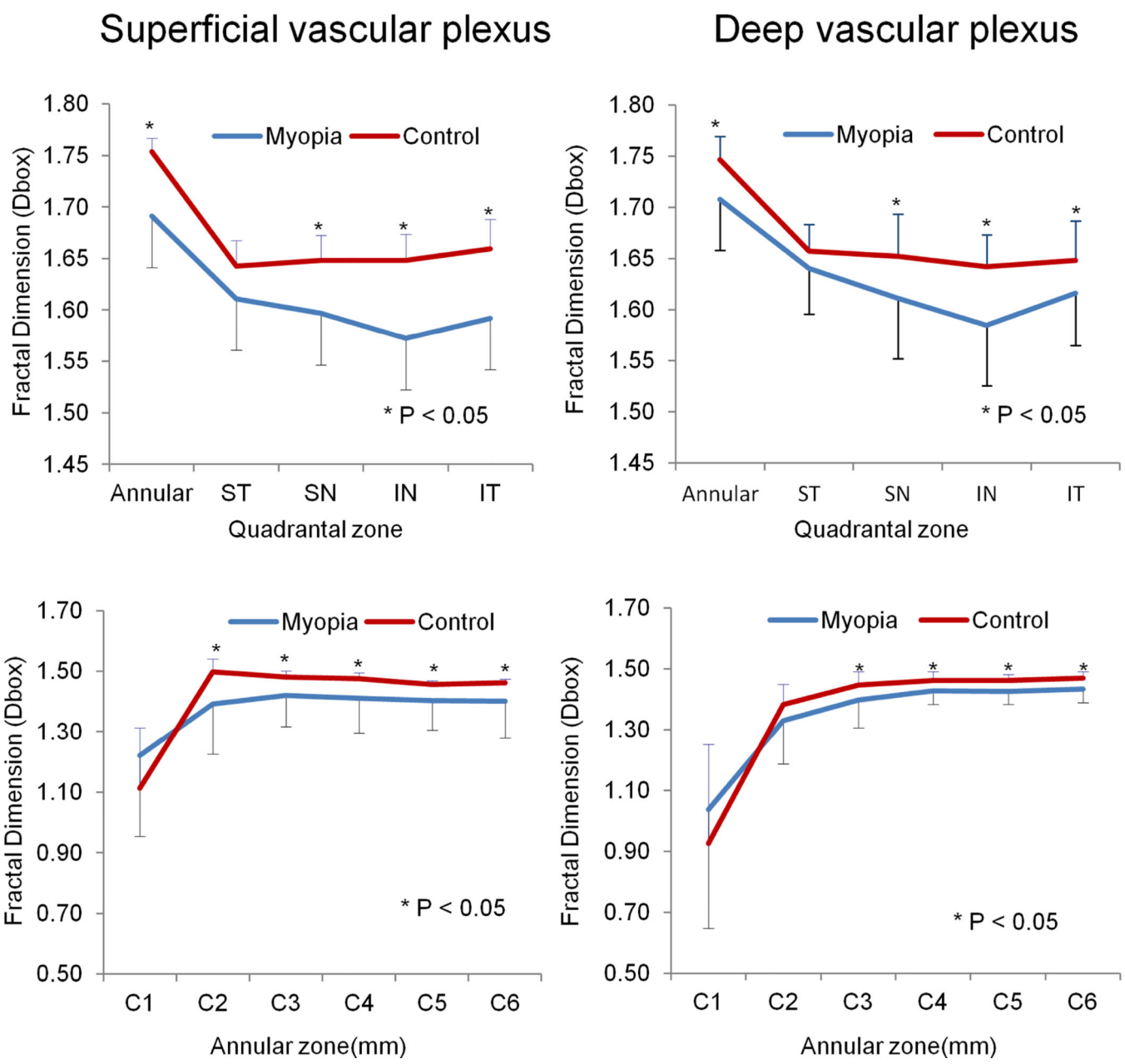

Fig. 5. Retinal microvascular density between the myopia subjects and the controls

Fractal analysis of the microvascular network was performed in each of the thin annuli and quadrants and fractal dimension (D_{box}) was obtained, representing vessel density. The microvessel densities of the annuli (from 0.6 to 2.5 mm in diameter) of both superficial and deep vascular plexuses were significantly lower in the myopia group than in the control group ($P < 0.01$, Fig. 5 upper left and right). Analysis of quadrantal partitions showed significant decreases in all quadrants in both plexuses, with the exception of the ST quadrant ($P < 0.05$, Fig. 5 upper left and right). The microvessel density in the thin annuli from C2 to C6 were significantly lower in the myopia group compared to the control group ($P < 0.05$, Fig. 5 bottom left and right), except for C2 in the deep vascular plexus. ST: Superior temporal, IT: inferior temporal, SN: superior nasal, IN: inferior nasal.

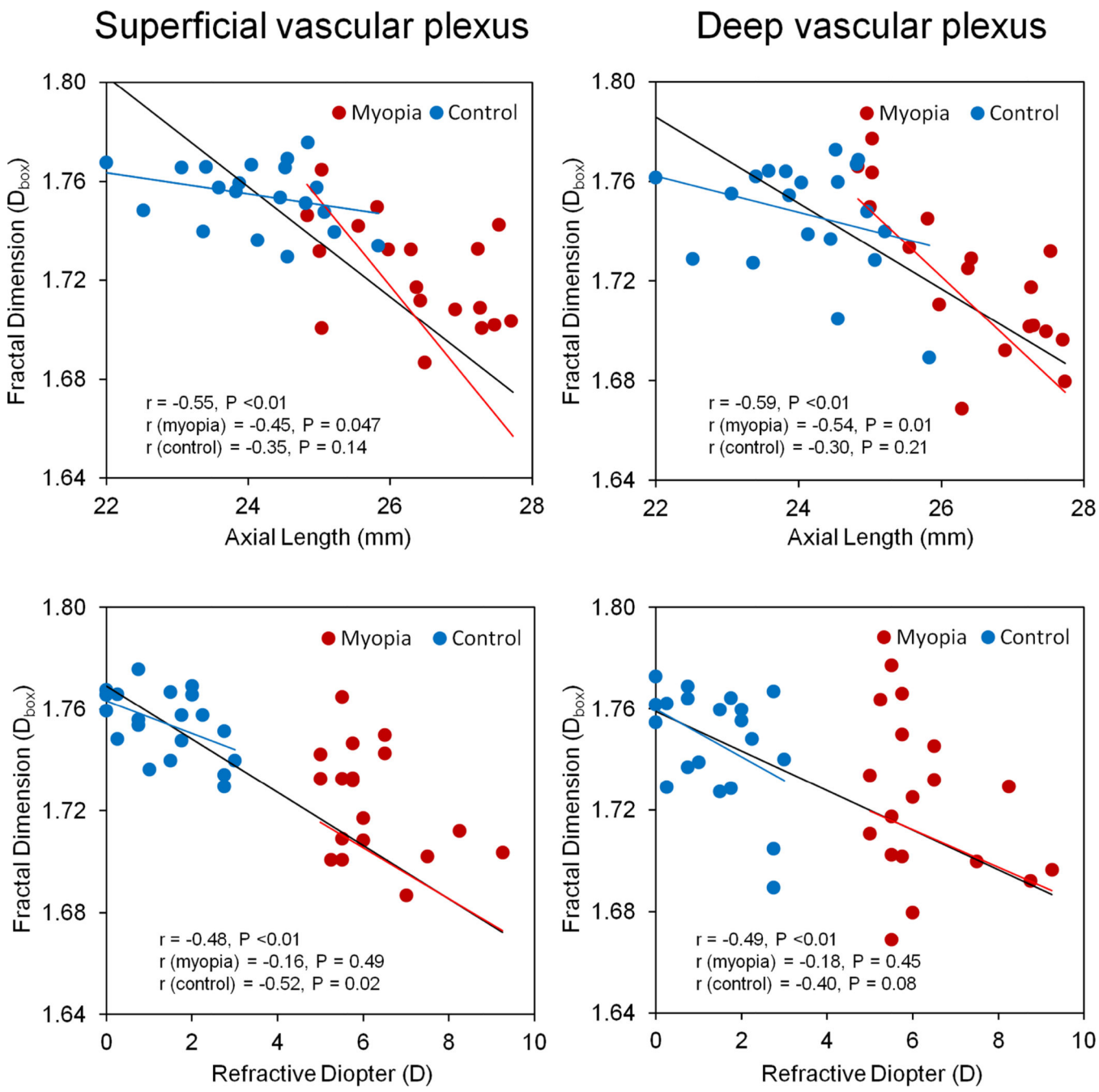

Fig. 6. Relationship between retinal microvascular density and axial length and refraction

Microvascular density in both superficial and deep vascular plexuses was negatively correlated with AL and refractive diopters when the results of both groups were combined. When the densities were analyzed separately, microvascular densities in both superficial (r = −0.45, P = 0.047, Fig. 6 upper left) and deep (r = −0.54, P = 0.01, Fig. 6 upper right) vascular plexuses were negatively correlated with the axial lengths in the myopic eye. Interestingly, microvascular densities in the superficial vascular plexus (r = −0.52, P = 0.02,

Fig. 6 bottom left) was negatively correlated to the refractive diopter in the control group. The black line in each panel denotes the regression line for combining both groups.

Table 1

Demographic and clinical information

	Myopia (mean ± SD)	Control (mean ± SD)	P value
Sample size	20 eyes	20 eyes	-
Gender	15 females, 5 males	13 females, 7 males	0.49
Age (years, mean ± SD)	28 ± 5	30 ± 6	0.38
Refractory error (D)	−6.31 ± 1.23	−1.40 ± 1.00	< 0.01
Axial Length(mm)	26.44 ± 0.97	24.13 ± 0.95	< 0.01
Systolic Blood Pressure (SBP, mmHg)	111.1 ± 9.4	114.1 ± 10.3	0.34
Diastolic Blood Pressure (DBP, mmHg)	73.0 ± 7.1	75.6 ± 9.3	0.32
Heart Rate (HR, bpm)	68.8 ± 11.5	71.7 ± 9.1	0.38

Table 2

Microvascular density (D_{box}) between myopia subjects and healthy controls in annular zones

Slabs	Group	Annulus	C1	C2	C3	C4	C5	C6
Superficial	Myopia	1.70 ± 0.07	1.21 ± 0.27	1.41 ± 0.12	1.43 ± 0.08	1.42 ± 0.07	1.41 ± 0.07	1.42 ± 0.06
Vascular	Normal	1.75 ± 0.01	1.11 ± 0.20	1.50 ± 0.04	1.48 ± 0.02	1.48 ± 0.02	1.46 ± 0.01	1.46 ± 0.01
Plexus	P value	< 0.01	0.12	< 0.01	< 0.01	< 0.01	< 0.01	< 0.02
Deep	Myopia	1.71 ± 0.05	1.07 ± 0.38	1.34 ± 0.14	1.40 ± 0.09	1.43 ± 0.04	1.43 ± 0.04	1.44 ± 0.04
Vascular	Normal	1.75 ± 0.02	0.93 ± 0.33	1.38 ± 0.07	1.45 ± 0.04	1.46 ± 0.03	1.46 ± 0.02	1.47 ± 0.02
Plexus	P value	< 0.01	0.12	0.10	0.03	< 0.01	< 0.01	< 0.01

Table 3

Microvascular density between myopia subjects and healthy controls in quadrants

Slabs	Group	ST	SN	IN	IT
Superficial	Myopia	1.62 ± 0.07	1.61 ± 0.07	1.58 ± 0.08	1.60 ± 0.09
Vascular	Normal	1.64 ± 0.02	1.65 ± 0.02	1.65 ± 0.03	1.66 ± 0.03
Plexus	P value	0.10	0.01	< 0.01	< 0.01
Deep	Myopia	1.64 ± 0.04	1.61 ± 0.06	1.59 ± 0.06	1.62 ± 0.05
Vascular	Normal	1.66 ± 0.03	1.65 ± 0.04	1.64 ± 0.03	1.65 ± 0.04
Plexus	P value	0.09	< 0.01	< 0.01	0.02